Elucidating Oxygen Reduction Active Sites in Pyrolyzed Metal-Nitrogen Coordinated Non-Precious Electrocatalyst Systems.

Urszula Tylus[a], Qingying Jia[a], Kara Strickland[a], Nagappan Ramaswamy[a, #], Alexey Serov[b],

Plamen Atanassov[b] and Sanjeev Mukerjee[a]*

[a] Northeastern University Center for Renewable Energy Technology, Department of Chemistry and Chemical Biology, Northeastern University, 317 Egan Research Center, 360 Huntington Avenue, Boston, MA 02115 USA

Author Present Address: General Motors Global Fuel Cell Activities, 895 Joslyn Avenue, Pontiac, MI 48340, USA

[b] Department of Chemical and Nuclear Engineering, 1 University of New Mexico, University of New Mexico, Albuquerque, NM 87131, USA

Table S1: Electrochemical parameters of carbon supported polymer-metal composites-PVAG-Fe and xBPEI-Fe and developed by UNM Fe-8AAPyr with the sacrificial support method whose high performance has been previously reported by Serov et al[1], compared to Tanaka Pt/C. (RDE in 0.1M $HClO_4$: Scan rate: 20mV/s. Loading of MNC catalysts: 0.6mg/cm^2 on 5.61mm glassy carbon disc electrode. Loading of Pt/C: catalyst 25µg$_{Pt}$/cm^2

Catalyst	Tafel slope [mV/decade]	i_{lim} [mA/cm^2]	i @ 0.8V (vs. RHE) [mA/cm^2]
30%Pt/C, 25µg/cm^2	61	4.4	3.6
UNM Fe8AAPyr, 0.6mg/cm^2	56	6.3	1.0
NEU PVAGFe, 0.6mg/cm^2	60	6.8	0.5
NEU xBPEIFe, 0.6mg/cm^2	58	5.6	0.4

Table S2: Potential dependent FT EXAFS fitting results of PVAG-Fe catalyst collected in-situ at Fe K-edge (7112eV) in O_2 saturated 0.1M $HClO_4$: Fitting results of theoretical FEFF8 calculations of the Fe-N$_x$/O peak, where CN = coordination number, and R = Fe-N bond length [Å].

Potential [V vs. RHE)	$CN_{Fe-N/O}$	R_{Fe-N} (Å)
0.3V	4.2+/-0.5	2.08+/-0.02
0.9V	4.9+/-0.8	2.05+/-0.02

Figure S1: ORR polarization curves at 0.12mg/cm^2 and 0.6mg/cm^2 catalyst loading in 0.1M HClO$_4$ (a) and 0.1M KOH (b), and c) RDE polarization curves of oxygen (ORR) and hydrogen peroxide (HRR) reduction in 0.1M HClO$_4$ (black) and 0.1 M KOH (blue) (RDE: RHE ref., GC 0.2472cm^2, 900rpm, 20mV-s and 0.6mg/cm^2 catalyst loading)
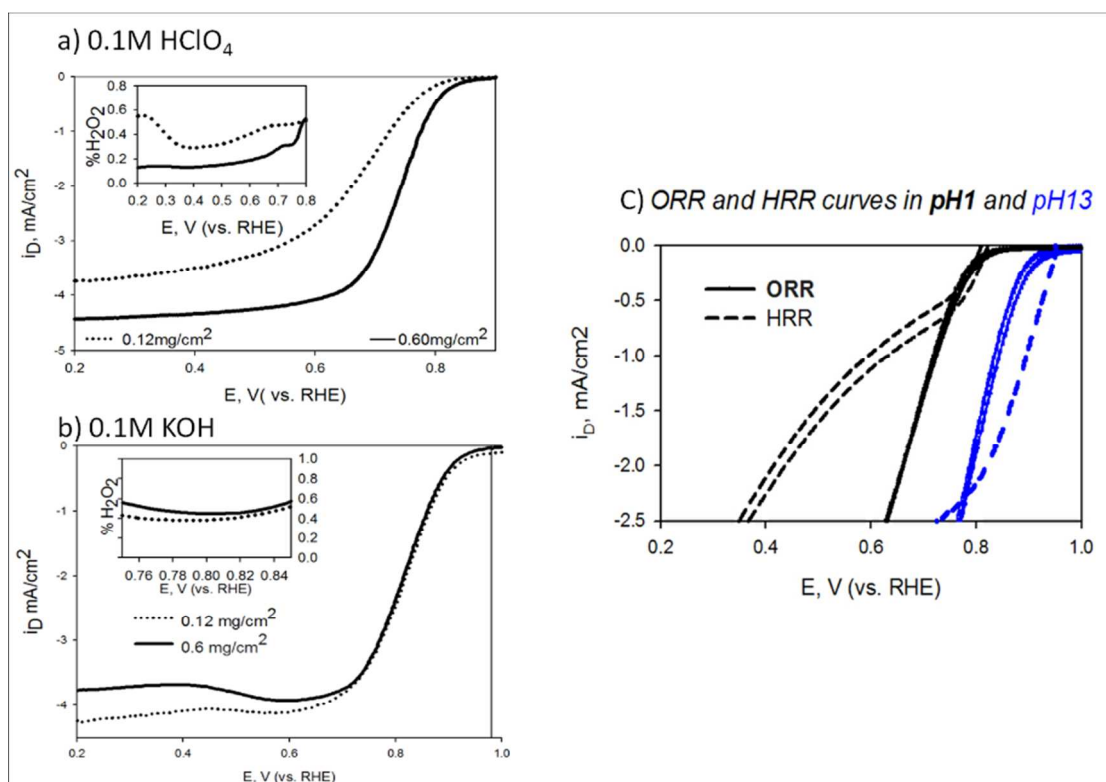
Figure S1a-b represents ORR polarization curves and yield of peroxide intermediate (as inset) in 0.1M $HClO_4$ (a) and 0.1M KOH (b). The improvement in kinetics with the loading observed in acid (Figure S2b), a typical behavior of pyrolyzed MNC's, is a result of increased density of active sites in the catalyst. The consistently low relative yield of peroxide intermediate (1%) even in low loading suggests that the PVAG-Fe catalyst facilitates ORR mainly through overall 4e mechanism. Considering however the apparent electron transferred between 3.2e-4e obtained by Koutecky-Levich at low and high loading respectively, the PVAG-Fe forms both water and peroxide as ORR final products suggesting 2x2e ORR mechanism. This discrepancy can be explained by disproportionation of some of the peroxide product before its further electroreduction know to occur in acid environment. On the hand, no change in kinetics upon increased catalyst loading in alkaline with the negligible yield of H_2O_2 (based on ring current and Koutecky-Levich equation) is consistent with true overall 4e ORR mechanism believed to take place in high pH media facilitated by catalyst with Fe-N_{2+2} type active centers [2,3]. Fe-N_{2+2} sites are able to facilitate efficient single site oxygen reduction to water through stabilization of peroxide intermediate (HO_2^-) on the catalytic surface (Figure S1c). The much smaller peroxide reduction currents in acid, suggest that only a small fraction of the intermediate undergo a direct reduction to water before it desorbs from the catalytic site. As already mentioned, the remaining H_2O_2 which detaches from the Fe center before its further reduction and is subjected to disproportionation or one-electron reduction [4] as shown below:

$$\underline{H_2O_2 \rightarrow H_2O + \tfrac{1}{2}\, O_2}\ (2)$$
$$Fe_{surf}{}^{2+} + H_2O_2 \rightarrow Fe_{surf}{}^{3+} + HO^{\bullet} + HO^{-}\ (2\text{-}1)$$
$$HO^{\bullet} + H_2O_2 \rightarrow HOO^{\bullet} + O_2\ (2\text{-}2)$$
$$HOO^{\bullet} + Fe_{surf}{}^{3+} + e^{-} \rightarrow Fe_{surf}{}^{2+} + H^{+} + O_2\ (2\text{-}2)$$
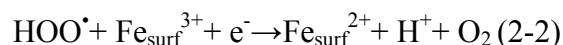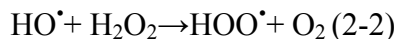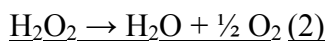
Figure S2: Effect of catalyst distortion on Koutecky-Levich plots (solid line represents initial performance, and dotted line represents post-treatment performance (a), and relative peroxide yield change versus level of Fe^0/Fe_xO_y destruction (b). The vertical red arrow indicates increase of peroxide yield with higher level of destruction as the concentration of the external H_2O_2 increased between 0, 0.03, 0.06, 0.12, 0.15 mmol/L (RRDE: 0.1M $HClO_4$, catalyst loading 0.12mg/cm^2).
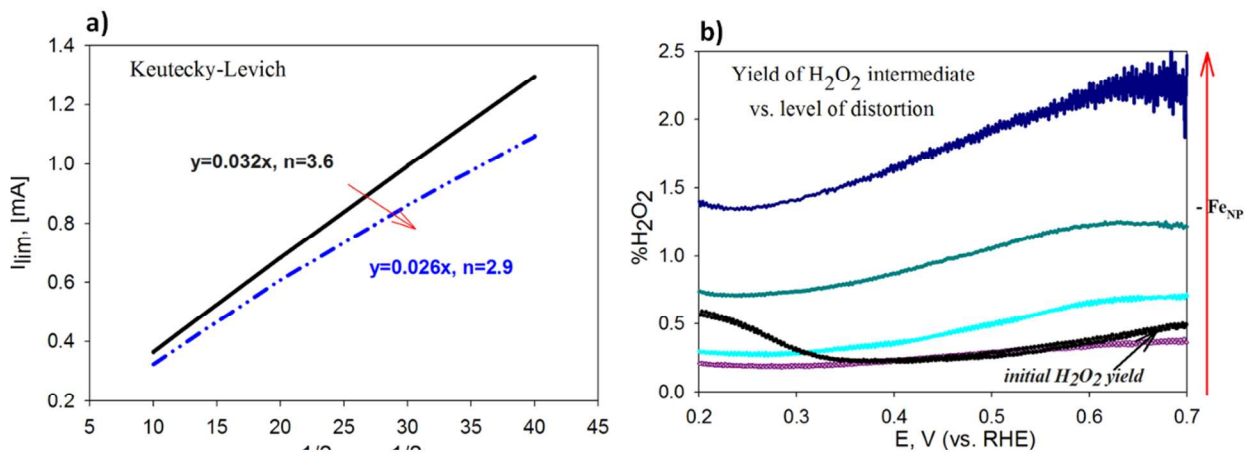
Figure S3: Theoretical XANES and delta-mu signatures of Fe-N$_4$C$_{10}$ and Fe-Fe janin cluster (representing Fe$_{NPs}$ when the O interacts with the Fe atom at fcc position) plotted individually (a), and as linear combination of the two (Fe-N$_4$C$_{10}$ /Fe$_{NPs}$) at various ratios (b). % of each of the Fe-forms in the PVAG-Fe was estimated by comparing ratio between the positive delta-mu features (cm$_{max1}$)/(cm$_{max2}$) of the experimental data with the theoretical delta-mu signatures of (c). The best agreement with the experimental delta mu signature was obtained with the theoretical model containing 93%Fe-N$_4$C$_{10}$+7%Fe$_{NPs}$ (shown in the main manuscript, Figure 4). Note that the structural models were utilized for delta-mu analysis using FEFF8 simulation. Theoretical Delta-mu signatures were obtained by subtracting the model XANES signatures according to $\Delta\mu(Fe\text{-}N_4C_{10}) = \mu(O\text{-}Fe\text{-}N_4C_{10}) - \mu(Fe\text{-}N_4C_{10})$; and $\Delta\mu(Fe_{NPs}) = \mu(O\text{-}Fe_{NPs}) - \mu(Fe_{NPs})$.
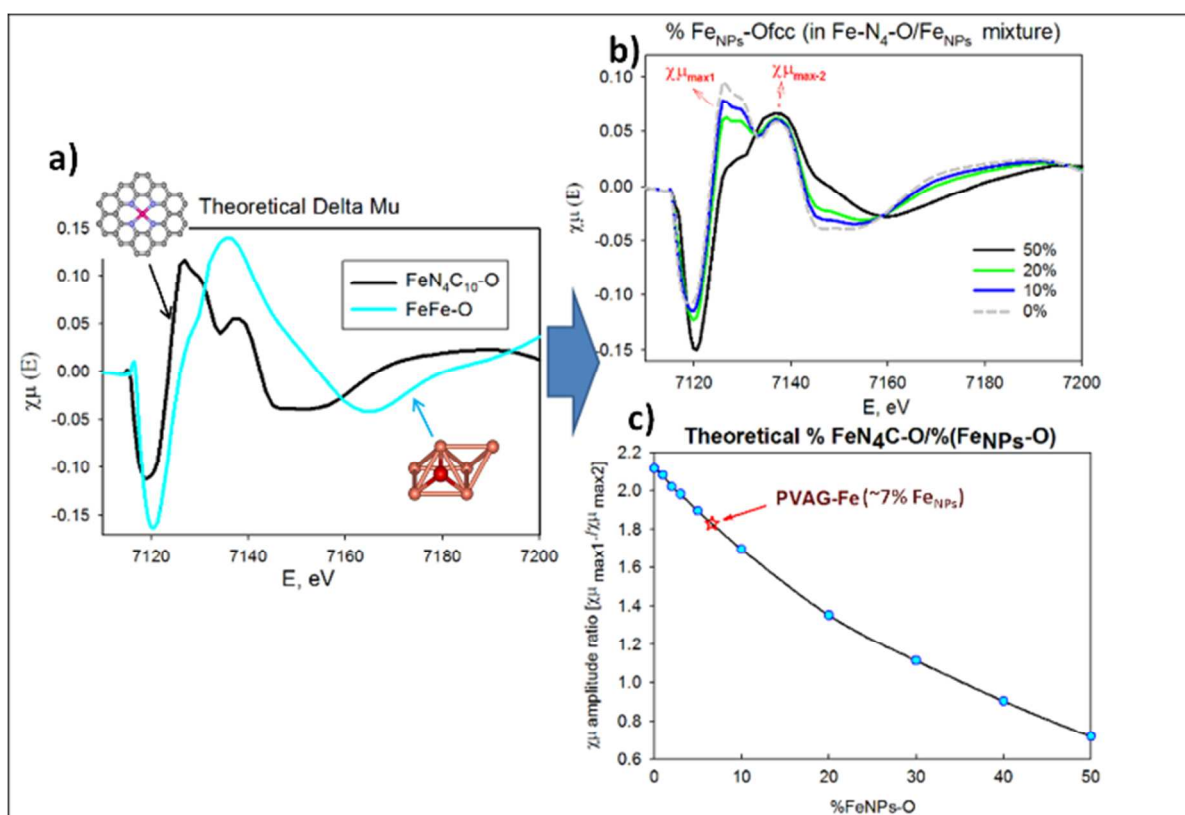
References:

(1)   Serov, A.; Robson, M. H.; Smolnik, M.; Atanassov, P. Templated Bi-Metallic Non-Pgm Catalysts for Oxygen Reduction *Electrochim. Acta* **2012**, *80*, 213-218.

(2)   Ramaswamy, N.; Mukerjee, S. Fundamental Mechanistic Understanding of Electrocatalysis of Oxygen Reduction on Pt and Non-Pt Surfaces: Acid Versus Alkaline Media *Adv. Chem. Phys.* **2012**, *2012*, 17.

(3)   Titov, A.; Zapol, P.; Král, P.; Liu, D.-J.; Iddir, H.; Baishya, K.; Curtiss, L. A. Catalytic Fe-Xn Sites in Carbon Nanotubes *The Journal of Physical Chemistry C* **2009**, *113*, 21629-21634.

(4)   Wiggins-Camacho, J. D.; Stevenson, K. J. Mechanistic Discussion of the Oxygen Reduction Reaction at Nitrogen-Doped Carbon Nanotubes *The Journal of Physical Chemistry C* **2011**, *115*, 20002-20010.